



Promotion of rs3746804 (p. L267P) polymorphism to intracellular SLC52A3a trafficking and riboflavin transportation in esophageal cancer cells

Lin Long¹ · Xiao-Xiao Pang^{1,2} · Fa-Min Zeng¹ · Xiu-Hui Zhan³ · Ying-Hua Xie¹ · Feng Pan¹ · Wei Wang¹ · Lian-Di Liao¹ · Xiu-E. Xu¹ · Bin Li⁴ · Li-Dong Wang⁵ · Zhi-Jie Chang⁶ · En-Min Li¹ · Li-Yan Xu¹ 

Received: 19 July 2020 / Accepted: 21 June 2021 / Published online: 5 July 2021
© The Author(s), under exclusive licence to Springer-Verlag GmbH Austria, part of Springer Nature 2021

Abstract

Riboflavin is an essential micronutrient for normal cellular growth and function. Lack of dietary riboflavin is associated with an increased risk for esophageal squamous cell carcinoma (ESCC). Previous studies have identified that the human riboflavin transporter SLC52A3a isoform (encoded by *SLC52A3*) plays a prominent role in esophageal cancer cell riboflavin transportation. Furthermore, *SLC52A3* gene single nucleotide polymorphisms rs3746804 (T>C, L267P) and rs3746803 (C>T, T278M) are associated with ESCC risk. However, whether SLC52A3a (p.L267P) and (p.T278M) act in riboflavin transportation in esophageal cancer cell remains inconclusive. Here, we constructed the full-length SLC52A3a protein fused to green fluorescent protein (GFP-SLC52A3a-WT and mutants L267P, T278M, and L267P/T278M). It was confirmed by immunofluorescence-based confocal microscopy that SLC52A3a-WT, L267P, T278M, and L267P/T278M expressed in cell membrane, as well as in a variety of intracellular punctate structures. The live cell confocal imaging showed that SLC52A3a-L267P and L267P/T278M increased the intracellular trafficking of SLC52A3a in ESCC cells. Fluorescence recovery after photobleaching of GFP-tagged SLC52A3a meant that intracellular trafficking of SLC52A3a-L267P and L267P/T278M was rapid dynamics process, leading to its stronger ability to transport riboflavin. Taken together, the above results indicated that the rs3746804 (p.L267P) polymorphism promoted intracellular trafficking of SLC52A3a and riboflavin transportation in ESCC cells.

Keywords SLC52A3a · Single nucleotide polymorphism · Riboflavin · Immunofluorescence · Esophageal cancer

Handling editor: D. Zilberstein.

Lin Long and Xiao-Xiao Pang contributed equally to this work.

✉ En-Min Li
nmli@stu.edu.cn

✉ Li-Yan Xu
lyxu@stu.edu.cn

¹ Institute of Oncologic Pathology, Department of Biochemistry and Molecular Biology, Shantou University Medical College, 22 Xinling Road, Shantou 515041, Guangdong, China

² Department of Pathology, Sun Yat-sen Memorial Hospital, Sun Yat-sen University, Guangzhou 510000, Guangdong, China

Introduction

With the largest population in the world, China's contribution to the global new cancer cases has exceeded 20% in recent years (Siegel et al. 2018). According to a cancer incidence and mortality report in China, esophageal cancer (EC)

³ Research Center of Translational Medicine, Department of Spine Surgery, The Second Affiliated Hospital of Shantou University Medical College, Shantou, Guangdong, China

⁴ State Key Laboratory of Luminescence and Applications, Changchun Institute of Optics, Fine Mechanics and Physics, Chinese Academy of Science, Changchun, China

⁵ Henan Key Laboratory for Cancer Research, The First Affiliated Hospital of Zhengzhou University, Zhengzhou, China

⁶ State Key Laboratory of Membrane Biology, School of Medicine, Tsinghua University, Beijing, China

is the fifth leading cause of cancer deaths (Chen et al. 2017). Esophageal squamous cell carcinoma (ESCC) is the predominant histological type of EC worldwide, which accounts for > 90% of all types of EC in China (Lin et al. 2013). The 5 year overall survival rate of patients with ESCC remains below 14% due to the lack of effective early detection biomarkers and early relapse warning biomarkers of ESCC (Lagergren and Mattsson 2012; Enzinger and Mayer 2003; Shimada et al. 2003). Therefore, it is imperative to develop efficient predictive and prognostic biomarkers of ESCC.

Previous reports indicated that lack of dietary riboflavin was associated with high risk of ESCC (Khan et al. 2011; He et al. 2009; Siassi and Ghadirian 2005; Zou et al. 2002). Human riboflavin transporter, SLC52A3a isoform (GenBank: AUI80409.1) encoded by the *SLC52A3* gene (Long et al. 2018b). As the most potent transporter of riboflavin (Long et al. 2018b; Yao et al. 2010), SLC52A3a isoform is frequently upregulated in ESCC patients, compared with normal adjacent tissue, and SLC52A3a could be used as both predictive and prognostic biomarker (Long et al. 2018b; Jiang et al. 2014; Fujimura et al. 2010; Yamamoto et al. 2009). Previous studies have shown that *SLC52A3* gene SNPs rs13042395 (C>T), rs3746803 (C>T), and rs3746804 (C>T), are associated with ESCC risk (Tan et al. 2016; Ji et al. 2011, 2012, 2014). Furthermore, rs13042395 located in the flanking region of the *SLC52A3* gene is a biomarker for regional lymph node metastasis and relapse-free survival in ESCC patients (Tan et al. 2016), while the rs3746804 (T>C, L267P) and rs3746803 (C>T, T278M), located in the coding region of *SLC52A3*, have been reported to be associated with tumor characteristics and survival in ESCC patients (Tan et al. 2016; Ji et al. 2011, 2012, 2014). However, little is known concerning the function of *SLC52A3* SNPs rs3746804 (T>C, L267P) and rs3746803 (C>T, T278M) variants at the riboflavin transportation in ESCC cells. In the present study, we hypothesize that the SNP rs3746804 (p. L267P) and rs3746803 (p. T278M) affect cancer progression by influencing SLC52A3a dynamics and riboflavin transportation in ESCC cells.

Therefore, we focused on the identification of functional SLC52A3a (p. L267P) and (p. T278M) variants, their associations with the riboflavin transportation in esophageal cancer cells. The 70 samples (29 cases with ESCC, matched noncancerous and muscle tissues) were collected and genotyped by whole-exon sequencing. The cellular localization of wild-type (WT) and mutated SLC52A3a was investigated by confocal immunofluorescence microscopy. Live cell confocal imaging was performed to observe the SLC52A3a intracellular trafficking and assess the riboflavin transportation capacity of WT and mutated SLC52A3a. Fluorescence recovery after photobleaching (FRAP) was used to evaluate the movement velocity of WT and mutated SLC52A3a. Genotype analysis showed that rs3746804 (TT genotypes, 267L)

and rs3746803 (TT genotypes, 278M) only existed in ESCC tissues, and that TT genotypes frequency of *SLC52A3* gene SNP rs3746804 (SLC52A3a-267L) was increased in ESCC tissues. Further live cell confocal imaging and FRAP demonstrated that rs3746804 (p.L267P) polymorphism increased SLC52A3a dynamics and promoted riboflavin intracellular trafficking in ESCC cells.

Materials and methods

SNPs identification and sequencing of the PCR products

Genotype analysis was performed on 70 samples resected from 29 patients (ESCC and matched noncancerous and muscle tissues) at Linzhou Cancer Hospital. All the surgical specimens were confirmed by pathological physicians, the noncancerous tissues were normal epithelium. Surgical specimens were prepared for frozen tissues. All the patients had not received radiotherapy or chemotherapy before operation. Information on gender, age, and histopathologic characteristics was obtained from the medical records. Patients' data are summarized in Supplemental Table 1. The studies involving human participants were reviewed and approved by the Ethics Committee of Shantou University Medical College (Institutional approval number: SUMC2013XM-0002). The patients provided their written informed consent to participate in this study.

Total DNA was extracted from frozen stored tissues of resected tumors of 29 ESCC patients (70 samples) using DNAzol reagent (Invitrogen) in accordance with the manufacturer's instructions. Primers for PCR are listed in Table 1. The PCR began with an initial denaturation step where samples were heated at 95 °C for 2 min, followed by denaturation at 95 °C for 30 s, annealing at 65 °C for 30 s and extension at 72 °C for 30 s in each cycle for 30 cycles, then final extension at 72 °C for 5 min. SNPs were identified by directly sequencing the PCR products using ABI Prism 2720 Sequence Detection System at the Beijing Genomic Center (BGI).

Human ESCC cell lines

Cell lines used in this study were previously described (Zeng et al. 2016; Lv et al. 2014). 1640 medium and riboflavin-free 1640 medium were purchased from Hyclone (Thermo Scientific, USA). Fetal bovine serum (FBS) was obtained from GIBCO (Life Technologies, USA). KYSE150 cells were cultured in 1640 medium (defined as KYSE150 R⁺) or riboflavin-free 1640 medium (defined as KYSE150 R⁻) media (Long et al. 2018a). All media were supplemented with 10% FBS and antibiotics (100 units/mL of penicillin

Table 1 Primers used in this study

Primer	Sequence (5'-3')
	Primers for SNPs identification
SLC52A3a-Exon3-F	GGAGTCCCAGAGCTTTGGT
SLC52A3a-Exon3-R	CTGTTAGGCAGGAACATGGAGA
	Primers for cloning
SLC52A3a-F	<u>GGATCC</u> ATTGGCCAGTTAGCGTGTC
SLC52A3a-R	GAATTCGCCGCACCTTGCATTTC
	Primers for mutagenesis
SLC52A3a-L267P-C-F	CCTCCACTCCATCCGG <u>CCG</u> CGGGAAGAGAATG
SLC52A3a-L267P-C-R	<u>GG</u> CCGGATGGAGTGGAGGGTGACCTGGTCA
SLC52A3a-T278M-T-F	CTTGGGCCCTGCAGGC <u>ATG</u> GTGGACAGCA
SLC52A3a-T278M-T-R	<u>ATG</u> CCTGCAGGGCCCAAGTCATTCTCTTC

F forward primer, *R* reverse primer

Cutting sites are underlined

The mutated sequence is in bold and shown as double underlined text

and 100 µg/mL of streptomycin). All cells were maintained at 37 °C in a humidified 5% CO₂ atmosphere.

Construction of GFP-tagged SLC52A3a expression plasmids

The coding region of SLC52A3a was amplified using the cloning primers listed in Table 1, after which they were ligated into the *Hind* III and *Bam*H I sites of pEGFP-C1 vector (Clontech) and verified by complete sequencing. A Fast Mutagenesis System Kit (TransGen Biotech, Beijing, China) was used to generate site-specific mutations, at leucine 267, threonine 278, according to the manufacturer's instructions. Detailed information about primers used for mutagenesis is listed in Table 1. Human KYSE150 esophageal carcinoma cells were transfected, with the GFP-SLC52A3a constructs, using Lipofectamine 3000 (Invitrogen) according to the manufacturer's instructions.

Western blotting

Whole cell protein extracts collected from cells were prepared in 1×Laemmli Sample Buffer (Bio-Rad), and proteins were separated on 10% SDS-PAGE and transferred to a PVDF membranes (Roche). The membranes were blocked in 5% non-fat milk for 1 h followed by the addition of the primary antibody (anti-GFP, SC-9996, Santa Cruz Biotechnology) for 1.5 h at room temperature. The membranes were then washed and incubated with a secondary antibody coupled to horseradish peroxidase for 1 h at room temperature. Antigen-antibody complexes were detected by Western blot luminol reagent (Santa Cruz Biotechnology). Image acquisition and quantitative analysis were carried out using the ChemiDoc XRS imaging system (Bio-Rad).

Immunofluorescence staining

The immunofluorescence staining was performed as described previously. Briefly, GFP-tagged SLC52A3a constructs were transfected into KYSE150 cells. After being fixed, permeabilized and blocked, cells were incubated with antibodies against GFP (Santa Cruz Biotechnology), then visualized with an Alexa Fluor 488-conjugated Affinipure donkey anti-mouse secondary antibody (Jackson ImmunoResearch). Followed by counterstaining with secondary antibodies, cells were incubated with 0.1 µg/mL DAPI (Sigma-Aldrich). Cells were analyzed using a Zeiss LSM880 confocal microscope (Zeiss).

Live cell confocal imaging and FRAP

GFP-tagged SLC52A3a constructs were transfected into KYSE150 cells. At 48 h post-transfection, the cells were inoculated into fibronectin-coated coverslips. Behavior of GFP-tagged SLC52A3a proteins in live cell was visualized using a confocal microscope LSM880 (Zeiss) with a 40×, 1.43NA, Plan-Apochromat oil objective (Zeiss). Fluorescence recovery after photobleaching (FRAP) (Day et al. 2012) was performed on a confocal microscope LSM880 (Zeiss). Cells were maintained at 37 °C on a heated stage. GFP-tagged proteins at the base and center of cell membrane were bleached in a rectangular region of area ranging from 1 to 3 µm² for ~0.5 s using the 488 nm and 543 nm laser lines at 100% laser power. Thereafter, fluorescence recovery within the bleached region was monitored every 1–3 s over a period of 45–60 s. The motion of individual trafficking vesicles was analyzed using MetaMorph tracking software (Molecular Devices, CN). Videos are provided as supplemental material (Supplemental Videos S1–8).

FRAP data were analyzed as follows. The average intensity in the bleached zone was measured over the time course of the experiment. The intensity of the bleached zone was corrected for photobleaching by multiplying a correction factor. We made curve fitting for the in vivo FRAP profile with a double-exponential function. Fluorescence recovery intensities curves were fitted using the following equation: $I(t) = I_{\text{END}} - I_1 \times e^{-\frac{t}{\tau_1}} - I_2 \times e^{-\frac{t}{\tau_2}}$, where $I(t)$ is the intensity of fluorescence at time t , I_1 is the intensity of fluorescence immediately post-bleaching, I_2 is the intensity of fluorescence following complete recovery (Day et al. 2012; Bancaud et al. 2010). Mobile fraction was calculated as the following formula: $M_f = (I_{\text{END}} - I_1) / (I_{\text{PRE}} - I_1)$, where I_{END} is the stable fluorescent intensity of the puncta after sufficient recovery, I_1 is the fluorescent intensity immediately after bleaching, and I_{PRE} is the fluorescent intensity before bleaching. The mobile fraction is the portion of molecules that can undergo diffusion. FRAP is a powerful, versatile, and widely accessible tool to monitor molecular dynamics in living cells. The mobile fraction rate can reflect the movement rate of membrane proteins on the cell membrane (Day et al. 2012). SLC52A3a acts as a riboflavin transporter, whose rapid distribution on the membrane can improve transmembrane transportation of riboflavin.

Riboflavin uptake assay

Both intra- or extra-cellular concentrations of riboflavin were measured by high-performance liquid chromatography (HPLC) as described previously (Petteys et al. 2011). Briefly, KYSE150 cells were plated at a density of 2×10^5 cells per well in 6-well plates, and culture medium was collected after 0 h, 24 h, 48 h, and 72 h respectively, while cells were collected after 72 h. The concentrations of riboflavin in the collected culture medium were measured directly by HPLC. KYSE150 Cells was lysed by ultrasonic wave, and riboflavin concentrations were measured by HPLC.

Statistical analysis

Data analysis were performed using SPSS 13.0 software and graphs were generated using GraphPad Prism 8.0. A two-tailed independent sample T test was used to determine the significance of differences between two groups. Differences among the multiple groups were analyzed using one-way ANOVA followed by Tukey's test (GraphPad Prism 8.0). Statistical significance was set at $P < 0.05$, $P < 0.05$ (*), $P < 0.01$ (**), $P < 0.001$ (***), $P < 0.0001$ (****), data are plotted as mean \pm SD.

Results

Exome sequencing identifies frequent mutation of the SLC52A3 gene in ESCC

To investigate the allele frequency in the exon region of the *SLC52A3* gene SNPs rs3746804 and rs3746803, we performed exon sequencing assay in 29 ESCC patients. As shown in Tables 2, 3 and 4, the comparative analysis of the sequencing results in ESCC, matched noncancerous and muscle tissues presents rs3746804 (TT genotypes, 267L) and rs3746803 (TT genotypes, 278 M) only existed in ESCC tissues, but not in matched noncancerous and muscle tissues. Notably, there were 41.38% CC genotypes and 58.62% TT genotypes in the genotype analysis of 29 patients with ESCC for rs3746804, while 82.76% CC genotypes and 17.24% TT genotypes for rs3746803, respectively. Then we searched the NCBI SNP database and found that the MAF (Minor Allele Frequency) of rs3746804 and rs3746803 were 18.23% (C>T) and 9.05% (C>T). Compared with our experimental results, the TT genotypes frequency of *SLC52A3* gene SNP rs3746804 was increased in ESCC tissues. Meanwhile, the TT genotypes frequency of *SLC52A3* gene SNP rs3746803 was also increased in ESCC tissues. These results suggest that *SLC52A3* gene SNP rs3746804 and rs3746803 TT genotypes have some associations with ESCC.

Table 2 Exon sequencing identifies *SLC52A3* SNP site in 29 ESCC patients

Name	SLC52A3a-L267P	SLC52A3a-T278M
dbSNP	rs3746804	rs3746803
Nucleotide position (NM_033409.4)	1139	1172
Nucleotide mutation	T \rightarrow C	C \rightarrow T
Amino acid position (NP_212134.3)	267	278
Amino acid mutation	Leu (L) \rightarrow Pro (P)	Thr (T) \rightarrow Met (M)
Allele frequency (%)		
C/C	41.38	82.76
T/T	58.62	17.24

Table 3 The exon sequencing assay results of 29 patients with ESCC

Sample ID	rs3746804 T→C (SLC52A3a-L267P)	rs3746803 T→C (SLC52A3a- T278M)
1322N	C	C
1322T	C	C
1336N	T	C
1336T	T	C
1339N	T	C
1339T	T	C
1357N	C	C
1357T	T	C
1395N	C	C
1395T	T	C
1405N	T	C
1405T	T	C
1430N	C	C
1430T	C	C
1432N	C	C
1432T	T	C
1443N	C	C
1443T	T	C
1445N	C	C
1445T	C	C
1469N	T	T
1469T	C	T
1481M	C	C
1481N	C	C
1481T	C	C
1486M	C	C
1486N	T	C
1486T	T	C
1527M	T	C
1527N	T	C
1527T	T	C
1550N	C	C
1550T	C	C
1569M	C	C
1569N	C	C
1569T	C	C
1572M	C	C
1572N	C	C
1572T	C	C
1582M	T	T
1582N	T	T
1582T	T	T
1618N	T	T
1618T	T	T
1642N	C	C
1642T	C	C
1652N	C	C

Table 3 (continued)

Sample ID	rs3746804 T→C (SLC52A3a-L267P)	rs3746803 T→C (SLC52A3a- T278M)
1652T	T	C
1665M	C	C
1665N	C	C
1665T	T	C
1706M	T	C
1706N	T	T
1706T	T	T
1708M	T	C
1708N	T	C
1708T	T	C
1805M	C	T
1805N	C	T
1805T	C	T
1829N	C	C
1829T	C	C
1859M	T	C
1859N	T	C
1859T	T	C
1867M	C	C
1867N	C	C
1867T	C	C
1868N	C	C
1868T	T	C

Localizations of GFP-SLC52A3a-WT, L267P, T278M, and L267P/T278M in human ESCC cells

To further investigate the above-mentioned SNP sites in ESCC, we constructed a GFP-tagged SLC52A3a plasmid and obtained several other mutants by mutation (See Method). SLC52A3a is a 469-amino acid protein, predicted to have 11 putative membrane-spanning domains by the SOSUI program (Hirokawa et al. 1998), as illustrated in Fig. 1A. Previously we have confirmed that SLC52A3a-WT (wild type, sequencing confirmed that amino acid positions 267 and 278 are leucine and threonine, respectively) expressed in cell membrane, cytoplasm and nucleus (Long et al. 2018b). To further confirm and compare the localizations of SLC52A3a mutants, we examined the sub-cellular localizations of GFP-SLC52A3a-WT, L267P, T278M, and L267P/T278M in KYSE150 cells. Western blot analysis confirmed successful over-expressions of GFP-SLC52A3a proteins (Fig. 1B). Positive staining for GFP-SLC52A3a was observed in all KYSE150 cells including cells transfected with GFP-SLC52A3a-WT, L267P, T278M, and L267P/T278M. Consistent with previous results, SLC52A3a was detectable in all sub-cellular

Table 4 Comparing the sequencing results in 29 cases with ESCC, matched noncancerous, and muscle tissues

Tissue type	rs3746804 T → C (SLC52A3a-L267P)	rs3746803 C → T (SLC52A3a-T278M)
Tumor	CC (41.38%), TT (58.62%)	CC (82.76%), TT (17.24%)
Adjacent non-tumor	CC (100.0%), TT (0.00%)	CC (100.0%), TT (0.00%)
Muscle	CC (100.0%), TT (0.00%)	CC (100.0%), TT (0.00%)

compartments, including cell membrane, cytoplasm as well as nucleus (Fig. 1C).

The dynamics of GFP-SLC52A3a-WT, L267P, T278M, and L267P/T278M with or without riboflavin in human ESCC cells

Previously, we have found that the SLC52A3a protein isoform encoded by the *SLC52A3* gene is responsible for the transport of riboflavin transport in esophageal cancer cells. To explore the effect of SNP locus on the ability of SLC52A3a to transport riboflavin, we next sought to investigate the dynamics of GFP-SLC52A3a-WT, L267P, T278M, and L267P/T278M with or without riboflavin in human ESCC cell line models. We photobleached GFP-SLC52A3a-WT, L267P, T278M, and L267P/T278M fluorescence in the membrane of KYSE150 R⁺ and R⁻ cells and examined the fluorescence recovery dynamic using Fluorescence Recovery After Photobleaching (FRAP). The mobile fraction values were also presented. We found that L267P and L267P/T278M promoted recovery of GFP fluorescence of SLC52A3a in the membrane of KYSE150 R⁺ and R⁻ cells within 60 s (Fig. 2A, B). Furthermore, the mobile fraction of GFP-SLC52A3a-L267P and GFP-SLC52A3a-L267P/T278M in cell membrane of KYSE150 R⁺ and R⁻ cells were also significantly increased compared with GFP-SLC52A3a-WT (Fig. 2C). Meanwhile, the recovery of GFP-SLC52A3a showed no difference between T278M and WT form in GFP fluorescence recovery and Mobile Fraction. These data suggest that L267P increased SLC52A3a dynamics and promoted riboflavin transmembrane transportation.

Intracellular trafficking of GFP-SLC52A3a-WT, L267P, T278M, and L267P/T278M in living cells

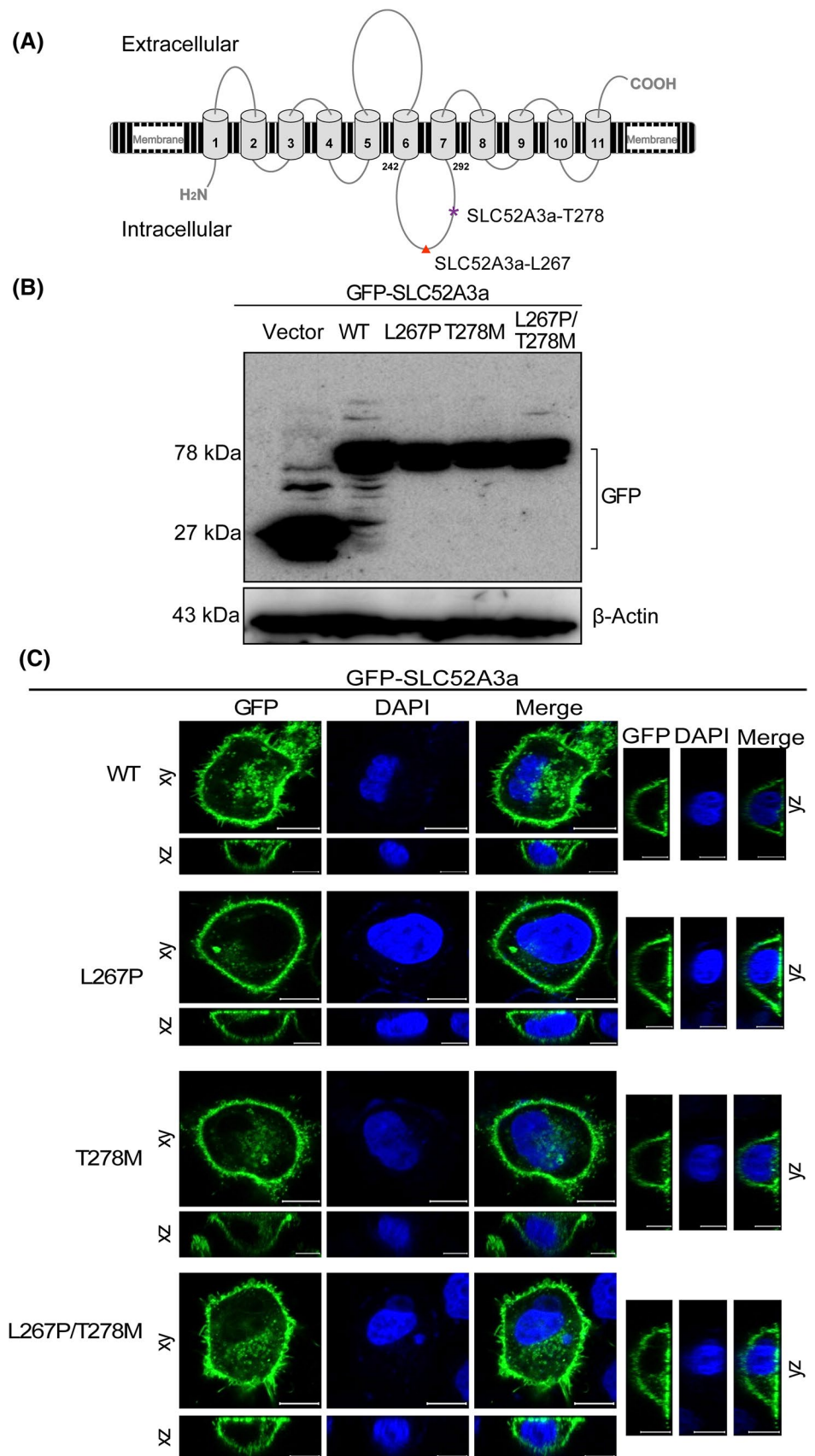
Since WT SLC52A3a and mutant SLC52A3a (L267P, T278M or L267P/T278M) can affect dynamics, we suspect that these mutations may affect the transportation of riboflavin in ESCC cells. Confocal immunofluorescence microscopy showed that the WT SLC52A3a and mutant SLC52A3a expressed in cell membrane, as well as in a variety of intracellular punctate structures, congruent with previous observations (Subramanian et al. 2011) (Fig. 1C).

To investigate the dynamics of individual trafficking vesicles in intracellular trafficking of WT SLC52A3a and mutant SLC52A3a to the cell membrane, we used live cell confocal imaging to track the motility of individual structures in the vesicle population. Results showed that the velocity of vesicle movements in GFP-SLC52A3a-L267P and GFP-SLC52A3a-L267P/T278M significantly increased compared to SLC52A3a-WT in KYSE150 R⁺ cells. In contrast, expression of GFP-SLC52A3a-L267P and GFP-SLC52A3a-L267P/T278M did not significantly cause alterations in KYSE150 R⁻ cells, while expression of GFP-SLC52A3a-T278M significantly decreased vesicle movements velocity (Fig. 3B, left and middle panel, Supplemental Videos S1–8). Intriguingly, when compared overall vesicle movements velocity in KYSE150 R⁺ and R⁻ cells, the vesicle movements mean velocity of GFP-SLC52A3a-WT, L267P, and L267P/T278M in cell membrane of KYSE150 R⁻ cells were also significantly increased compared with KYSE150 R⁺ cells, while we found that the vesicle movements mean velocity of GFP-SLC52A3a-T278M in KYSE150 R⁻ cells did not show any significant change between KYSE150 R⁺ cells (Fig. 3B, right panel). These data suggest that SLC52A3a-L267P increases the intracellular trafficking of SLC52A3a.

Transport capacity of riboflavin by SLC52A3a -WT, L267P, T278M, and L267P/T278M in human ESCC cells

We next sought to investigate the transport capacity of riboflavin by SLC52A3a-WT and mutants using ESCC cell line KYSE150. We have measured both riboflavin consumption in cell culture medium and intracellular riboflavin concentration using high-performance liquid chromatography (HPLC). Importantly, our results showed that cells expressing SLC52A3a-L267P exhibited faster riboflavin consumption and maintained higher intracellular concentration of riboflavin compared to SLC52A3a-WT cells (Fig. 3C). These data suggesting that SLC52A3a-L267P has higher capacity in transporting riboflavin than SLC52A3a-WT.

Fig. 1 Subcellular localization of GFP-tagged SLC52A3a in ESCC cell lines by immunofluorescence analysis. **A** Topology of SLC52A3a. Transmembrane domains were predicted by the SOSUI program. Position of the 267-leucine residue is marked by red triangle. Position of the 278-threonine residue is marked by purple star. **B** Western blot analysis of GFP-tagged SLC52A3a transfected into KYSE150 cells. Data shown are representative of two independent experiments. **C** Immunofluorescence analysis of GFP-SLC52A3a in KYSE150 cells. The GFP-tagged SLC52A3a were labeled with Alexa Fluor 488 (green) and nuclei were counterstained with DAPI (blue). Bar = 10 μ m. Experiments were repeated three times with similar results



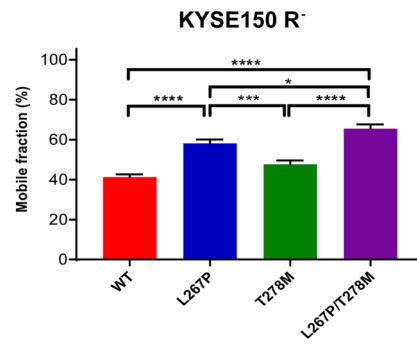
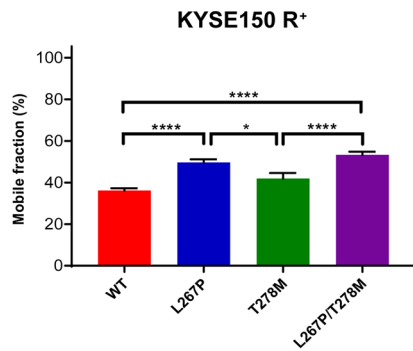
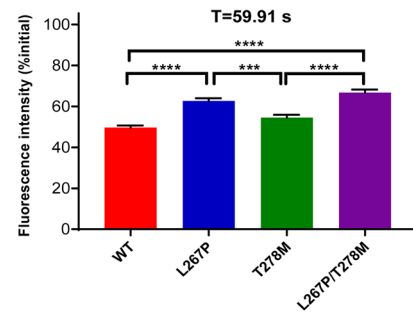
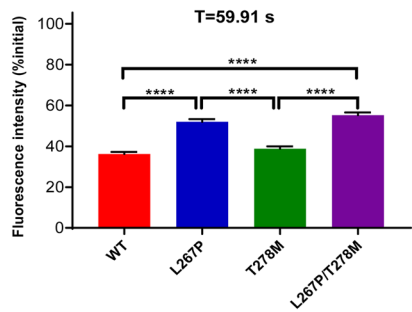
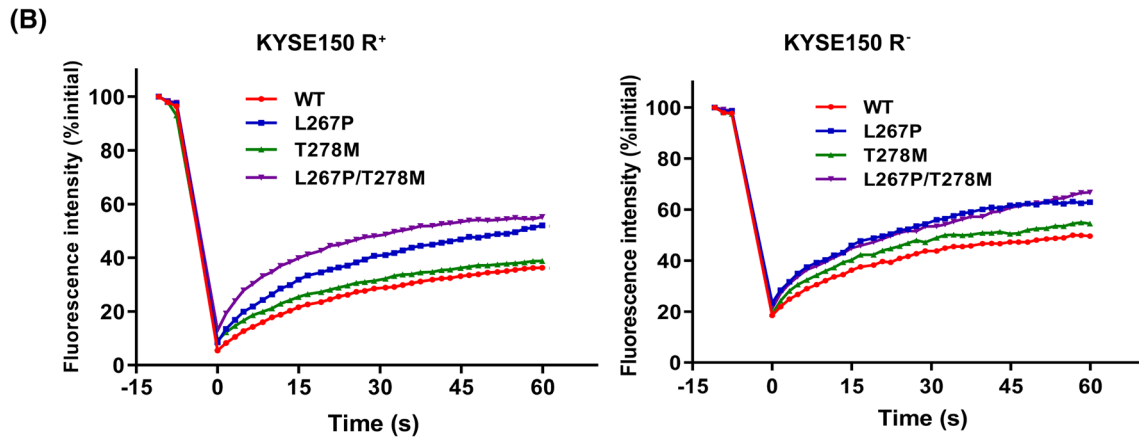
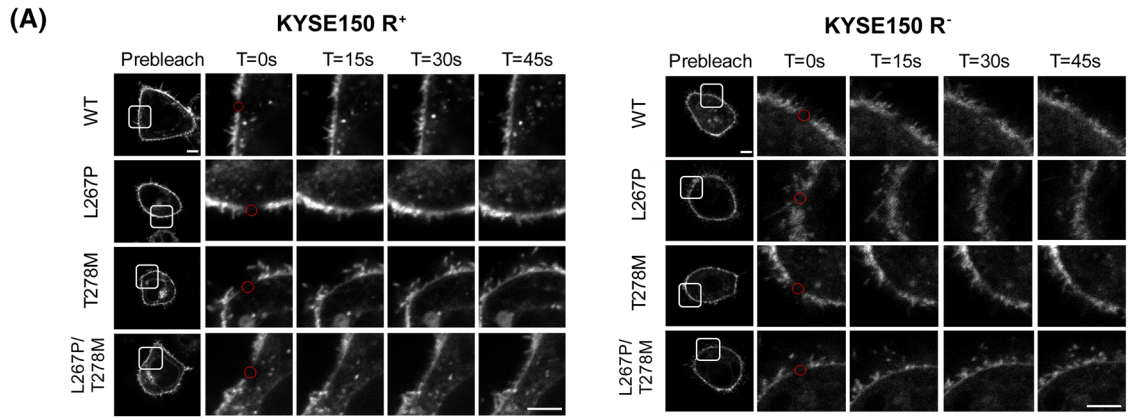


Fig. 2 Comparison of FRAP data for different GFP-SLC52A3a proteins in riboflavin normal or riboflavin deficiency KYSE150 cell membrane. **A** The representative images of FRAP were shown and the selected areas were measured for fluorescence recovery after photobleaching. Bar=5 μ m. **B** Recovery curves for SLC52A3a-WT (red circles), SLC52A3a-L267P (blue squares), SLC52A3a-T278M (green triangles), and SLC52A3a-L267P/T278M (purple inverted triangles) in the membrane of KYSE150 cells. Data show the mean recoveries for 30 cells for each protein from a representative experiment. The above data were analyzed by one-way ANOVA, followed by Tukey's test, T (time)=59.91 s, **** P <0.0001, *** P <0.001. **C**, Summarized data of the mobile fractions (M_p) of SLC52A3a-WT (red), SLC52A3a-L267P (blue), SLC52A3a-T278M (green), and SLC52A3a-L267P/T278M (purple) in KYSE150 cells. The above data were analyzed by one-way ANOVA, followed by Tukey's test. **** P <0.0001, *** P <0.001, * P <0.05. Error bars indicate SD, n =30 cells. The experiments were performed independently in triplicate. R^+ riboflavin normal; R^- riboflavin deficiency

Discussion

The SNP has been shown to be associated with tumor progression in various malignancies (Zhang et al. 2018; Briones-Orta et al. 2017; Johnson et al. 2016). Previous studies on SNP indicated that the polymorphisms in the exon coding regions can directly influence the functional properties of the proteins and the mutations may be associated with different responsiveness to cancer therapies and patients' survival (Srinivasan et al. 2019; Katiyar et al. 2017; Wagner et al. 2010). The SNP rs3746804 and rs3746803 in the exon coding region of *SLC52A3* gene identified might be as susceptibility locus of ESCC (Ji et al. 2011, 2012). In this study, we investigated whether the SNP rs3746804 and rs3746803 alleles could affect the SLC52A3a protein expression and regulating riboflavin transportation in ESCC cells. The rs3746804, SLC52A3a 267P, is proline endopeptidase cleavage site. The rs3746803, SLC52A3a 278T, is a site of modification by protein kinase C. Our study indicated that the SLC52A3a-L267P increased SLC52A3a dynamics and promoted riboflavin transmembrane transportation. Simultaneously, SLC52A3a-L267P and T278M increased the intracellular trafficking of SLC52A3a. Together with our results, these findings indicating that the SLC52A3a-L267P might play a prominent role in riboflavin transportation in ESCC.

SLC52A3a is a crucial riboflavin transporter, involved in cell uptake of riboflavin (Long et al. 2018b; Yang et al. 1982, 1984; Thurnham et al. 1982; Groenewald et al. 1981). Riboflavin deficiency has been identified as a risk factor for ESCC (Khan et al. 2011; Zou et al. 2002; Siassi and Ghadirian 2005). Previous research indicates that riboflavin supplementation can reduce the incidence of ESCC (He et al. 2009; Dawsey et al. 1994; Blot et al. 1993). However, blood riboflavin in 34% of the riboflavin supplemented ESCC patients was still lower than normal (He et al. 2009). These findings suggest that the lack of riboflavin in ESCC patients is not only related to the concentration of riboflavin in the environment but also to riboflavin transporters. Our findings indicated that the SNP rs3746804 (p. L267P) could increase the intracellular trafficking of SLC52A3a and promote riboflavin transportation in ESCC cells according to the live cell confocal imaging and FRAP results. Notably, our exon sequencing results showed that the TT genotypes frequency of *SLC52A3* gene SNP rs3746804 was significantly increased in ESCC (TT genotypes, SLC52A3a amino acid 267 site is leucine). We speculate SLC52A3a L267 frequency increased and SLC52A3a P267 frequency decreased in ESCC, which lead to weaker riboflavin transportation capacity and promote cancer progression.

There are still some limitations in our findings. In our experiment, we found that the rs3746804 (p.L267P) could increase the intracellular trafficking of SLC52A3a and promote riboflavin transportation in ESCC cells, while the deeper insight into the molecular mechanisms involved in SLC52A3a-L267P affecting riboflavin transportation still need to be investigated in future studies.

Conclusion

In summary, we identified that the SNP rs3746804 (p. L267P) in SLC52A3a was closely related to SLC52A3a dynamics and riboflavin transportation in ESCC cells. The rs3746804 (p.L267P) could increase the intracellular trafficking of SLC52A3a and promote riboflavin transportation in ESCC cells (Fig. 4). These results provided some new choices for clinical research of ESCC and targeted therapy.

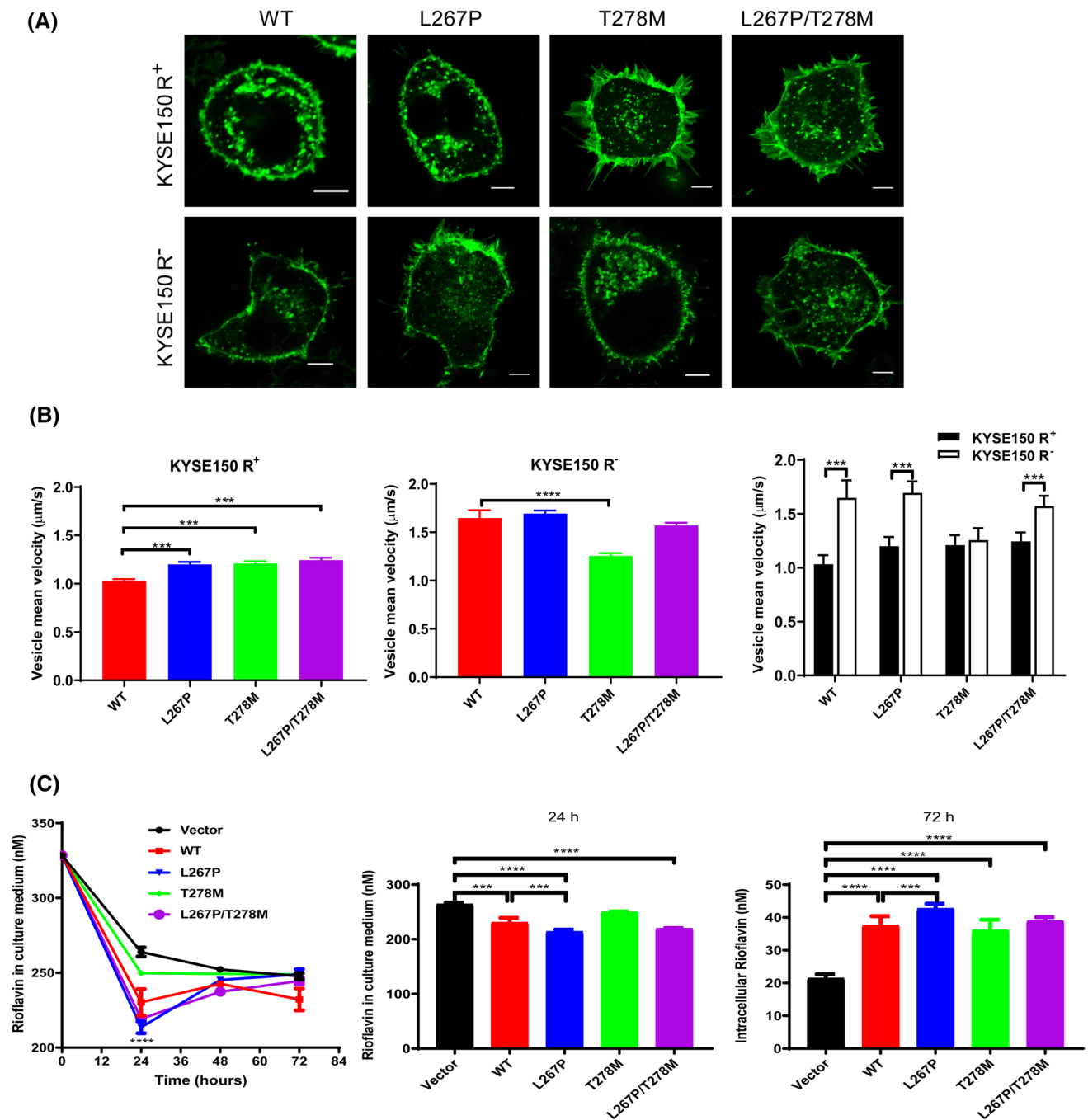


Fig. 3 Intracellular trafficking of GFP-SLC52A3a-WT, L267P, T278M and L267P/T278M in living cells. **A** Distribution of GFP-SLC52A3a trafficking vesicles in KYSE150 R⁺ and R⁻ cells. Bar=5 µm. **B** Average velocity of GFP-SLC52A3a trafficking vesicles was observed in KYSE150 R⁺ and R⁻ cells maintained at 37 °C. Data are from 266 vesicles. Data are means±SD of at least three separate determinations. The above data were analyzed by one-way ANOVA, followed by Tukey's test. **** $P < 0.0001$, *** $P < 0.001$. **C** Concentrations of riboflavin in culture medium and intracellularly were quantified by HPLC. The concentrations of riboflavin in

culture medium after KYSE150 cells were transfected with vector, SLC52A3a-WT or mutants for 0 h, 24 h, 48 h and 72 h (*left*). The concentrations of riboflavin in culture medium after KYSE150 cells were transfected with vector, SLC52A3a-WT or mutants for 24 h (*middle*). The intracellular riboflavin concentrations in KYSE150 after being transfected with vector, SLC52A3a-WT or mutants for 72 h (*right*). The value was an average of three times repeats, and error bars indicate S.D. **** $P < 0.0001$, *** $P < 0.001$ based on one-way ANOVA, followed by Tukey's test. R⁺ riboflavin normal, R⁻ riboflavin deficiency

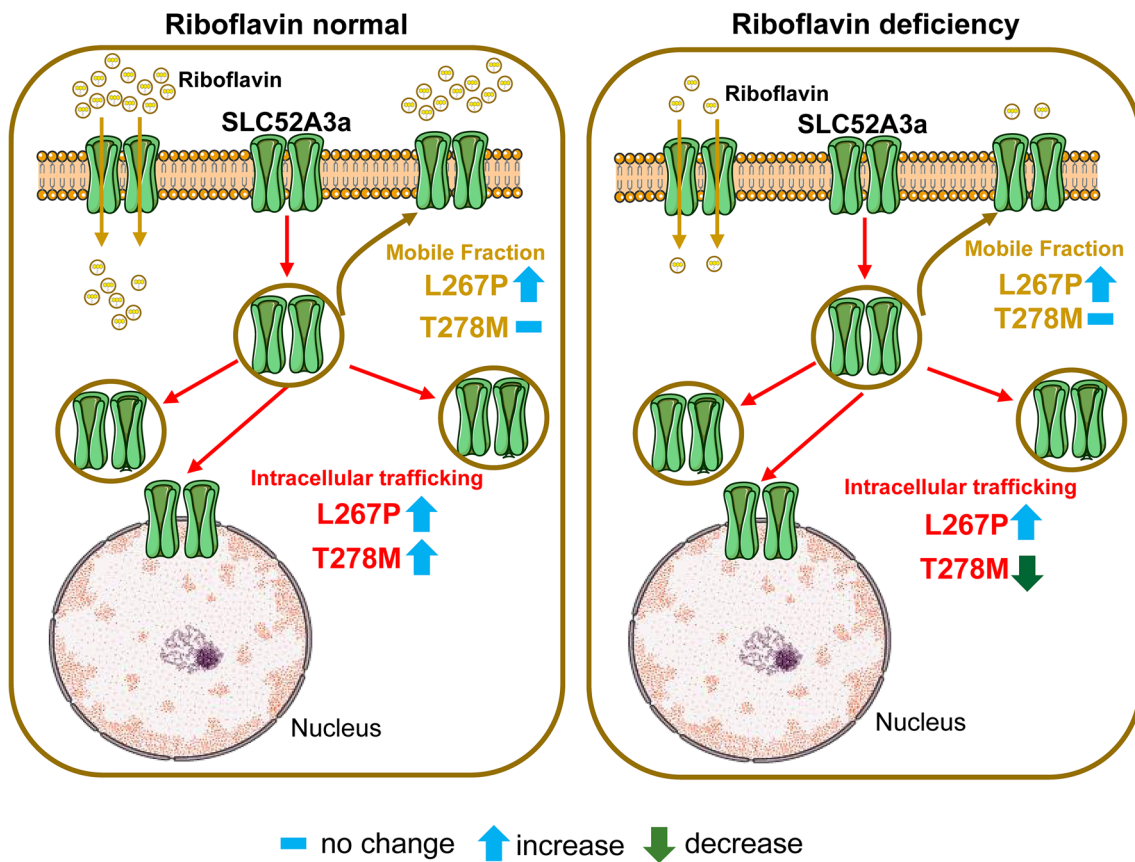


Fig. 4 Schematic model of the association of SLC52A3a [p. L267P] and [p. T278M] with riboflavin transportation in ESCC cells

Supplementary Information The online version contains supplementary material available at <https://doi.org/10.1007/s00726-021-03025-4>.

Author contributions LL: data collection, data analysis, and drafting; LYX, EML, BL, LDW, and ZJC: study design, study supervision, and final approval of the manuscript; XXP, FMZ, XHZ, and YHX: immunofluorescence staining, live cell confocal imaging, and FRAP; FP and XEX: sample collection; WW: SNPs identification; LDL: cell culture.

Funding This study was supported by grants from Natural Science Foundation of China-Guangdong Joint Fund (U1301227); The National Natural Science Foundation of China (82002975, 81772532 and 81472613); The Foundation for Young Talents in Higher Education of Guangdong (2018KQNCX085); and The Science and Technology Developing Project of Jilin Province, Grant/Award Number: 20180101176JC.

Declarations

Conflict of interest The authors declare no conflict of interest.

Ethics statement The studies involving human participants were reviewed and approved by the Ethics Committee of Shantou University Medical College (Institutional approval number: SUM-C2013XM-0002). The patients provided their written informed consent to participate in this study. All procedures performed in studies involving the human participant were in accordance with the ethical

standards of the institutional and/or national research committee and with the 1964 Helsinki declaration and its later amendments or comparable ethical standards.

References

- Bancaud A, Huet S, Rabut G, Ellenberg J (2010) Fluorescence perturbation techniques to study mobility and molecular dynamics of proteins in live cells: FRAP, photoactivation, photoconversion, and FLIP. *Cold Spring Harb Protoc* 2010(12):90. <https://doi.org/10.1101/pdb.top90>
- Blot WJ, Li JY, Taylor PR, Guo W, Dawsey S, Wang GQ, Yang CS, Zheng SF, Gail M, Li GY et al (1993) Nutrition intervention trials in Linxian, China: supplementation with specific vitamin/mineral combinations, cancer incidence, and disease-specific mortality in the general population. *J Natl Cancer Inst* 85(18):1483–1492
- Briones-Orta MA, Avendano-Vazquez SE, Aparicio-Bautista DI, Coombes JD, Weber GF, Syn WK (2017) Osteopontin splice variants and polymorphisms in cancer progression and prognosis. *Biochim Biophys Acta Rev Cancer* 1868:93–108. <https://doi.org/10.1016/j.bbcan.2017.02.005>
- Chen W, Zheng R, Zhang S, Zeng H, Xia C, Zuo T, Yang Z, Zou X, He J (2017) Cancer incidence and mortality in China, 2013. *Cancer Lett* 401:63–71. <https://doi.org/10.1016/j.canlet.2017.04.024>

- Dawsey SM, Wang GQ, Taylor PR, Li JY, Blot WJ, Li B, Lewin KJ, Liu FS, Weinstein WM, Wiggett S et al (1994) Effects of vitamin/mineral supplementation on the prevalence of histological dysplasia and early cancer of the esophagus and stomach: results from the Dysplasia Trial in Linxian. *China Cancer Epidemiol Biomarkers Prev* 3(2):167–172
- Day CA, Kraft LJ, Kang M, Kenworthy AK (2012) Analysis of protein and lipid dynamics using confocal fluorescence recovery after photobleaching (FRAP). *Curr Protoc Cytom Chapter 2*(Unit2):19. <https://doi.org/10.1002/0471142956.cy0219s62>
- Enzinger PC, Mayer RJ (2003) Esophageal cancer. *N Engl J Med* 349(23):2241–2252. <https://doi.org/10.1056/NEJMra035010>
- Fujimura M, Yamamoto S, Murata T, Yasujima T, Inoue K, Ohta KY, Yuasa H (2010) Functional characteristics of the human ortholog of riboflavin transporter 2 and riboflavin-responsive expression of its rat ortholog in the small intestine indicate its involvement in riboflavin absorption. *J Nutr* 140(10):1722–1727. <https://doi.org/10.3945/jn.110.128330>
- Groenewald G, Langenhoven ML, Beyers MJ, du Plessis JP, Ferreira JJ, van Rensburg SJ (1981) Nutrient intakes among rural Transkeians at risk for oesophageal cancer. *S Afr Med J Suid-Afrikaanse Tydskrif Vir Geneeskunde* 60(25):964–967
- He Y, Ye L, Shan B, Song G, Meng F, Wang S (2009) Effect of riboflavin-fortified salt nutrition intervention on esophageal squamous cell carcinoma in a high incidence area. *China Asian Pac J Cancer Prev* 10(4):619–622
- Hirokawa T, Boon-Chiang S, Mitaku S (1998) SOSUI: classification and secondary structure prediction system for membrane proteins. *Bioinformatics* 14(4):378–379
- Ji A, Wang J, Yang J, Wei Z, Lian C, Ma L, Ma L, Chen J, Qin X, Wang L, Wei W (2011) Functional SNPs in human C20orf54 gene influence susceptibility to esophageal squamous cell carcinoma. *Asian Pac J Cancer Prev* 12(12):3207–3212
- Ji AF, Wei W, Yang JZ, Wang JS, Zhao L, Wei ZB, Lian CH, Ma L, Ma L, Wang HL, Qin XQ, Wang LD (2012) The relationship between C20orf54 gene rs3746804 position single nucleotide polymorphism and susceptibility to esophageal squamous cell carcinoma. *Zhonghua Nei Ke Za Zhi* 51(12):982–986
- Ji A, Ma L, Yang J, Xu Y, Wang J, Lian C, Wang Y, Li D, Dong WL, Wu W (2014) The functional SNP rs3746804 in C20orf54 modifies susceptibility to esophageal squamous cell carcinoma. *Oncol Res Treat* 37(11):654–657. <https://doi.org/10.1159/000368314>
- Jiang XR, Yu XY, Fan JH, Guo L, Zhu C, Jiang W, Lu SH (2014) RFT2 is overexpressed in esophageal squamous cell carcinoma and promotes tumorigenesis by sustaining cell proliferation and protecting against cell death. *Cancer Lett* 353(1):78–86. <https://doi.org/10.1016/j.canlet.2014.07.013>
- Johnson N, De Ieso P, Migliorini G, Orr N, Broderick P, Catovsky D, Matakidou A, Eisen T, Goldsmith C, Dudbridge F, Peto J, Dos-Santos-Silva I, Ashworth A, Ross G, Houlston RS, Fletcher O (2016) Cytochrome P450 allele CYP3A7*1C associates with adverse outcomes in chronic lymphocytic leukemia, breast, and lung cancer. *Cancer Res* 76(6):1485–1493. <https://doi.org/10.1158/0008-5472.CAN-15-1410>
- Katiyar T, Maurya SS, Hasan F, Singh AP, Khan AJ, Hadi R, Singh S, Bhatt MLB, Parmar D (2017) Association of cytochrome P450 1B1 haplotypes with head and neck cancer risk. *Environ Mol Mutagen* 58(6):443–450. <https://doi.org/10.1002/em.22098>
- Khan NA, Teli MA, Mohib-Ul Haq M, Bhat GM, Lone MM, Afroz F (2011) A survey of risk factors in carcinoma esophagus in the valley of Kashmir, Northern India. *J Cancer Res Ther* 7(1):15–18. <https://doi.org/10.4103/0973-1482.80431>
- Lagergren J, Mattsson F (2012) Diverging trends in recent population-based survival rates in oesophageal and gastric cancer. *PLoS ONE* 7(7):e41352. <https://doi.org/10.1371/journal.pone.0041352>
- Lin Y, Totsuka Y, He Y, Kikuchi S, Qiao Y, Ueda J, Wei W, Inoue M, Tanaka H (2013) Epidemiology of esophageal cancer in Japan and China. *J Epidemiol* 23(4):233–242
- Long L, He JZ, Chen Y, Xu XE, Liao LD, Xie YM, Li EM, Xu LY (2018a) Riboflavin depletion promotes tumorigenesis in HEK293T and NIH3T3 cells by sustaining cell proliferation and regulating cell cycle-related gene transcription. *J Nutr* 148(6):834–843. <https://doi.org/10.1093/jn/nxy047>
- Long L, Pang X-X, Lei F, Zhang J-S, Wang W, Liao L-D, Xu X-E, He J-Z, Wu J-Y, Wu Z-Y, Wang L-D, Lin D-C, Li E-M, Xu L-Y (2018b) SLC52A3 expression is activated by NF- κ B p65/Rel-B and serves as a prognostic biomarker in esophageal cancer. *Cell Mol Life Sci* 75(14):2643–2661. <https://doi.org/10.1007/s00018-018-2757-4>
- Lv GQ, Zou HY, Liao LD, Cao HH, Zeng FM, Wu BL, Xie JJ, Fang WK, Xu LY, Li EM (2014) Identification of a novel lysyl oxidase-like 2 alternative splicing isoform, LOXL2 Deltae13, in esophageal squamous cell carcinoma. *Biochem Cell Biol* 92(5):379–389. <https://doi.org/10.1139/bcb-2014-0046>
- Petteys BJ, Frank EL (2011) Rapid determination of vitamin B(2) (riboflavin) in plasma by HPLC. *Clin Chim Acta* 412(1–2):38–43. <https://doi.org/10.1016/j.cca.2010.08.037>
- Shimada H, Nabeya Y, Okazumi S, Matsubara H, Shiratori T, Gunji Y, Kobayashi S, Hayashi H, Ochiai T (2003) Prediction of survival with squamous cell carcinoma antigen in patients with resectable esophageal squamous cell carcinoma. *Surgery* 133(5):486–494. <https://doi.org/10.1067/msy.2003.139>
- Siassi F, Ghadirian P (2005) Riboflavin deficiency and esophageal cancer: a case control-household study in the Caspian Littoral of Iran. *Cancer Detect Prev* 29(5):464–469. <https://doi.org/10.1016/j.cdp.2005.08.001>
- Siegel RL, Miller KD, Jemal A (2018) Cancer statistics. *CA Cancer J Clin* 68(1):7–30. <https://doi.org/10.3322/caac.21442>
- Srinivasan S, Stephens C, Wilson E, Panchadsaram J, DeVoss K, Koistinen H, Stenman UH, Brook MN, Buckle AM, Klein RJ, Lilja H, Clements J, Batra J, Practical C (2019) Prostate cancer risk-associated single-nucleotide polymorphism affects prostate-specific antigen glycosylation and its function. *Clin Chem* 65(1):e1–e9. <https://doi.org/10.1373/clinchem.2018.295790>
- Subramanian VS, Rapp L, Marchant JS, Said HM (2011) Role of cysteine residues in cell surface expression of the human riboflavin transporter-2 (hRFT2) in intestinal epithelial cells. *Am J Physiol Gastrointest Liver Physiol* 301(1):G100–109. <https://doi.org/10.1152/ajpgi.00120.2011>
- Tan HZ, Wu ZY, Wu JY, Long L, Jiao JW, Peng YH, Xu YW, Li SS, Wang W, Zhang JJ, Li EM, Xu LY (2016) Single nucleotide polymorphism rs13042395 in the SLC52A3 gene as a biomarker for regional lymph node metastasis and relapse-free survival of esophageal squamous cell carcinoma patients. *BMC Cancer* 16:560. <https://doi.org/10.1186/s12885-016-2588-3>
- Thurnham DI, Rathakette P, Hambidge KM, Munoz N, Crespi M (1982) Riboflavin, vitamin A and zinc status in Chinese subjects in a high-risk area for oesophageal cancer in China. *Hum Nutr Clin Nutr* 36(5):337–349
- Wagner K, Damm F, Gohring G, Gorlich K, Heuser M, Schafer I, Ottmann O, Lubbert M, Heit W, Kanz L, Schlomok G, Raghavachar AA, Fiedler W, Kirchner HH, Bruggen W, Zucknick M, Schlegelberger B, Heil G, Ganser A, Krauter J (2010) Impact of IDH1 R132 mutations and an IDH1 single nucleotide polymorphism in cytogenetically normal acute myeloid leukemia: SNP rs11554137 is an adverse prognostic factor. *J Clin Oncol* 28(14):2356–2364. <https://doi.org/10.1200/JCO.2009.27.6899>
- Yamamoto S, Inoue K, Ohta KY, Fukatsu R, Maeda JY, Yoshida Y, Yuasa H (2009) Identification and functional characterization of rat riboflavin transporter 2. *J Biochem* 145(4):437–443. <https://doi.org/10.1093/jb/mvn181>

- Yang CS, Miao J, Yang W, Huang M, Wang T, Xue H, You S, Lu J, Wu J (1982) Diet and vitamin nutrition of the high esophageal cancer risk population in Linxian. *China Nutr Cancer* 4(2):154–164. <https://doi.org/10.1080/01635588209513751>
- Yang CS, Sun Y, Yang QU, Miller KW, Li GY, Zheng SF, Ershow AG, Blot WJ, Li JY (1984) Vitamin A and other deficiencies in Linxian, a high esophageal cancer incidence area in northern China. *J Natl Cancer Inst* 73(6):1449–1453
- Yao Y, Yonezawa A, Yoshimatsu H, Masuda S, Katsura T, Inui K (2010) Identification and comparative functional characterization of a new human riboflavin transporter hRFT3 expressed in the brain. *J Nutr* 140(7):1220–1226. <https://doi.org/10.3945/jn.110.122911>
- Zeng FM, Xie YM, Liao LD, Li LY, Chen B, Xie JJ, Xu LY, Li EM (2016) Biological characterization of three immortalized esophageal epithelial cell lines. *Mol Med Rep* 14(5):4802–4810. <https://doi.org/10.3892/mmr.2016.5813>
- Zhang B, Zhou J, Liu Z, Gu L, Ji J, Kim WH, Deng D (2018) Clinical and biological significance of a—73A > C variation in the CDH1 promoter of patients with sporadic gastric carcinoma. *Gastric Cancer* 21(4):606–616. <https://doi.org/10.1007/s10120-017-0778-6>
- Zou XN, Taylor PR, Mark SD, Chao A, Wang W, Dawsey SM, Wu YP, Qiao YL, Zheng SF (2002) Seasonal variation of food consumption and selected nutrient intake in Linxian, a high risk area for esophageal cancer in China. *Int J Vitam Nutr Res* 72(6):375–382

Publisher's Note Springer Nature remains neutral with regard to jurisdictional claims in published maps and institutional affiliations.